Supplementary Information (SI) for Journal of Materials Chemistry A.
This journal is © The Royal Society of Chemistry 2025

Supplementary Information

Simultaneously Enhancing Charge Transport and Analyte Accessibility in Poly(3-hexylthiophene) Transistors *via* Highly π-π Stacking Nanowire Network for Ammonia Sensing

Tianqing Miao,[a] Hongjiao Wang,[a] Cancan Li,[a] Deyu Bao,[a] Yujin Li,[a] Shenwei Wu,[a] Junhuai Wang,[a] Yidi Zhou,[a] Chenfang Sun[a] and Xiao Li*[a]*

[a] Tianjin Key Laboratory of Life and Health Detection, Life and Health Intelligent Research Institute, Tianjin University of Technology, Tianjin 300384, P. R. China.

*Corresponding authors: sunchenfang@email.tjut.edu.cn; lixiao@email.tjut.edu.cn

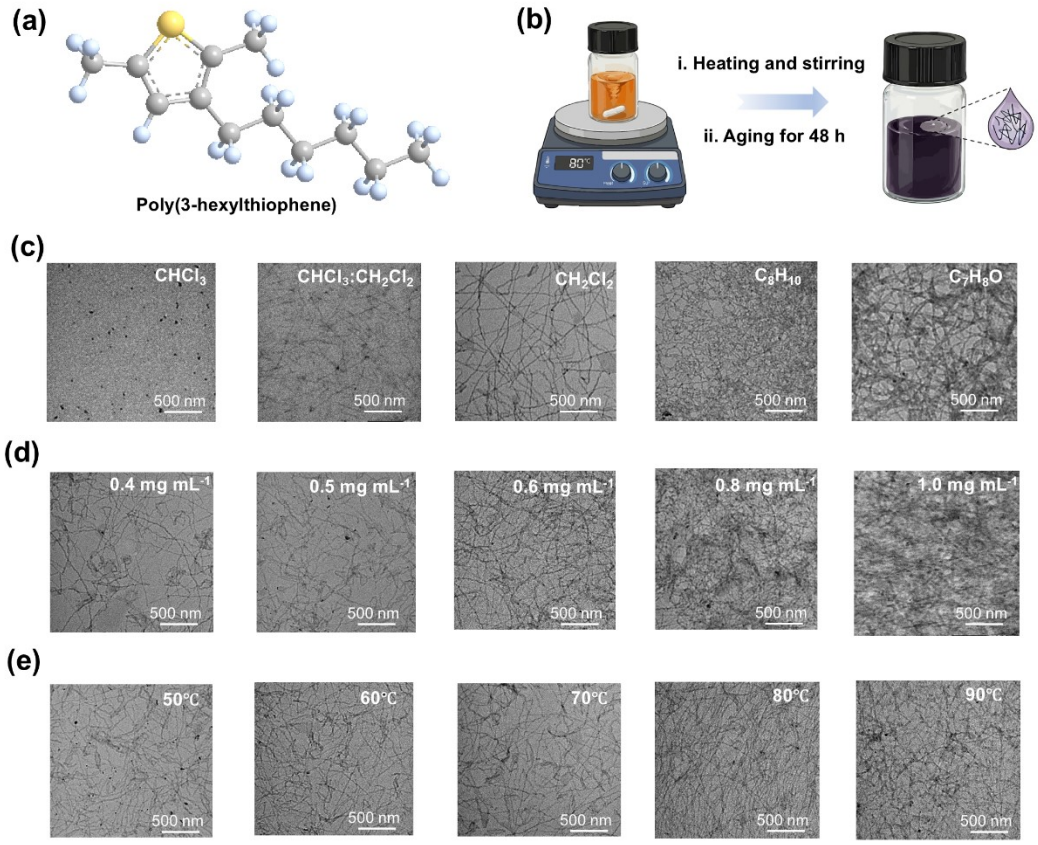

Fig. S1. Morphological evolution of P3HT nanostructures regulated by a solvent-concentration-temperature ternary regulation strategy. (a) chemical structure of P3HT, (b) schematic illustration of P3HT NW fabrication process via solution cooling method: (i) heating and stirring to ensure complete dissolution of P3HT; (ii) aging the solution at room temperature for 48 h, (c) effect of different solvents on the microstructure of P3HT (chloroform, chloroform and dichloromethane, dichloromethane, p-xylene, and anisole), (d) effect of different P3HT concentrations on nanowire morphology in dichloromethane (0.4 mg mL^{-1}, 0.5 mg mL^{-1}, 0.6 mg mL^{-1}, 0.8 mg mL^{-1}, and 1.0 mg mL^{-1}), (e) effect of different dissolution temperatures on nanowire morphology in dichloromethane (50℃, 60℃, 70℃, 80℃, and 90℃).

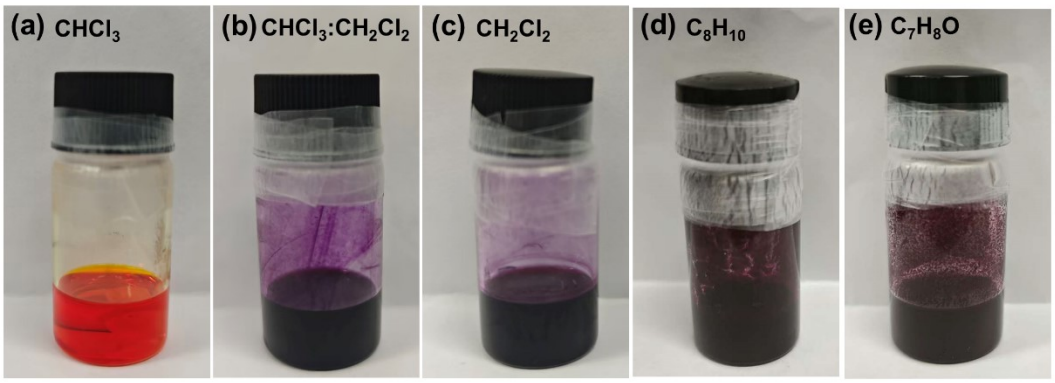

Fig. S2. P3HT solutions prepared with different solvents. (a) chloroform ($CHCl_3$), (b) chloroform and dichloromethane ($CHCl_3$:CH_2Cl_2), (c) dichloromethane (CH_2Cl_2), (d) p-xylene (C_8H_{10}), and (e) anisole (C_7H_8O).

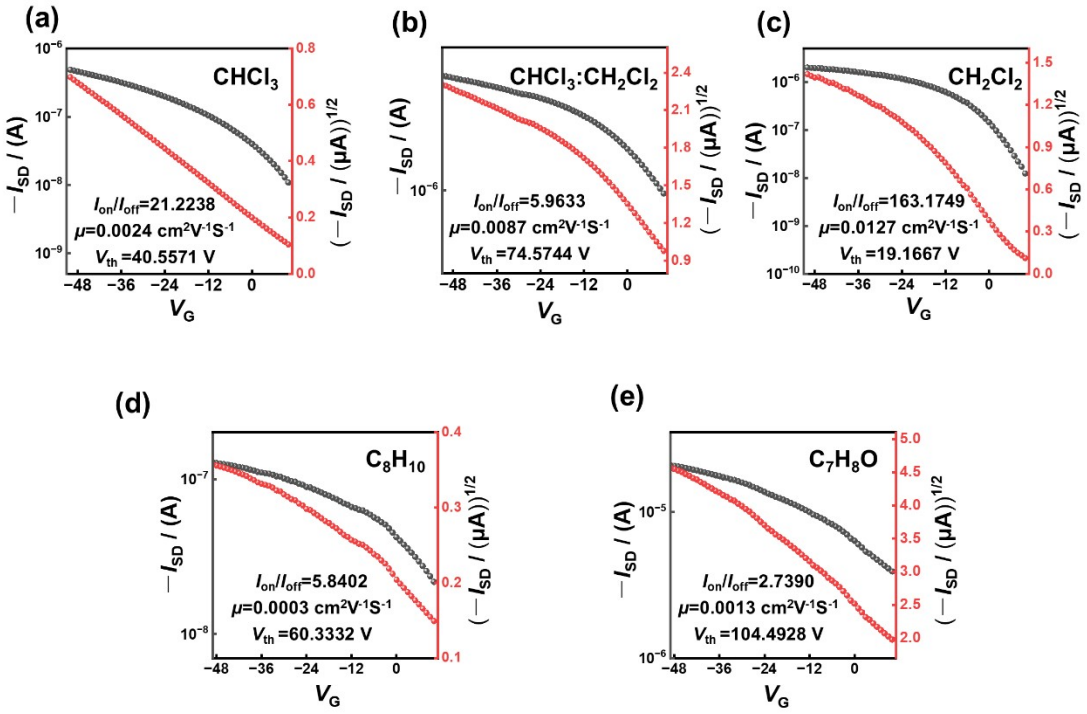

Fig. S3. Transfer curves of different solvents on the OTFTs based on P3HT NW. (a) chloroform ($CHCl_3$), (b) chloroform and dichloromethane ($CHCl_3$:CH_2Cl_2), (c) dichloromethane (CH_2Cl_2), (d) p-xylene (C_8H_{10}), and (e) anisole (C_7H_8O).

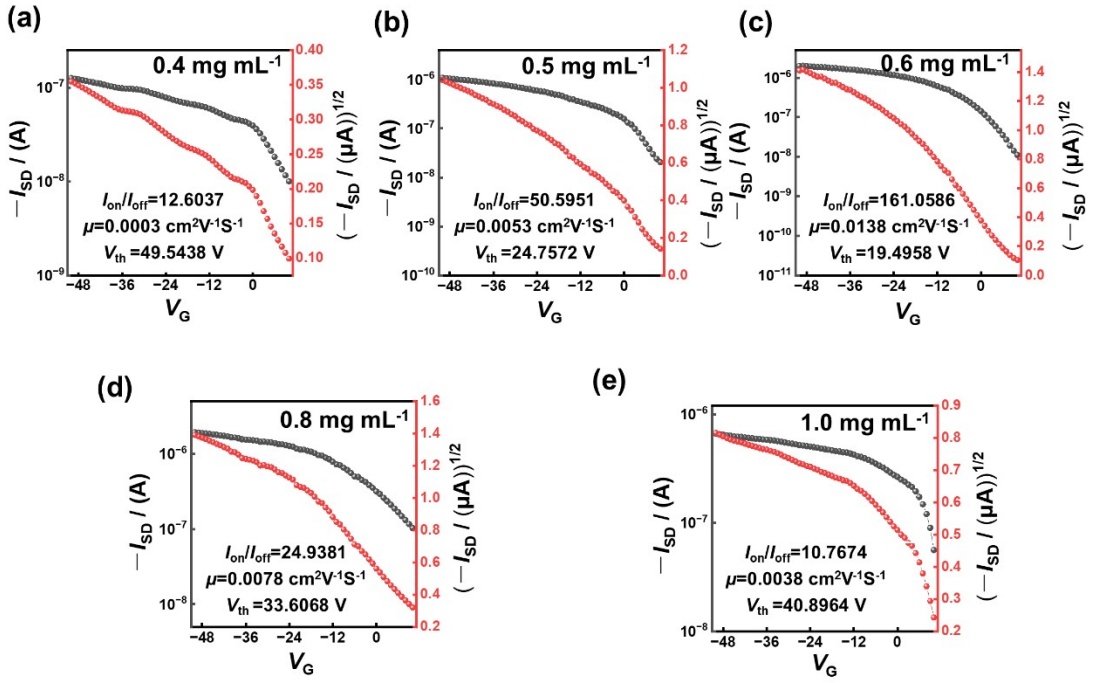

Fig. S4. Transfer curves of different concentrations in dichloromethane on the OTFTs based on P3HT NW. (a) 0.4 mg mL^{-1}, (b) 0.5 mg mL^{-1}, (c) 0.6 mg mL^{-1}, (d) 0.8 mg mL^{-1}, and (e) 1.0 mg mL^{-1}.

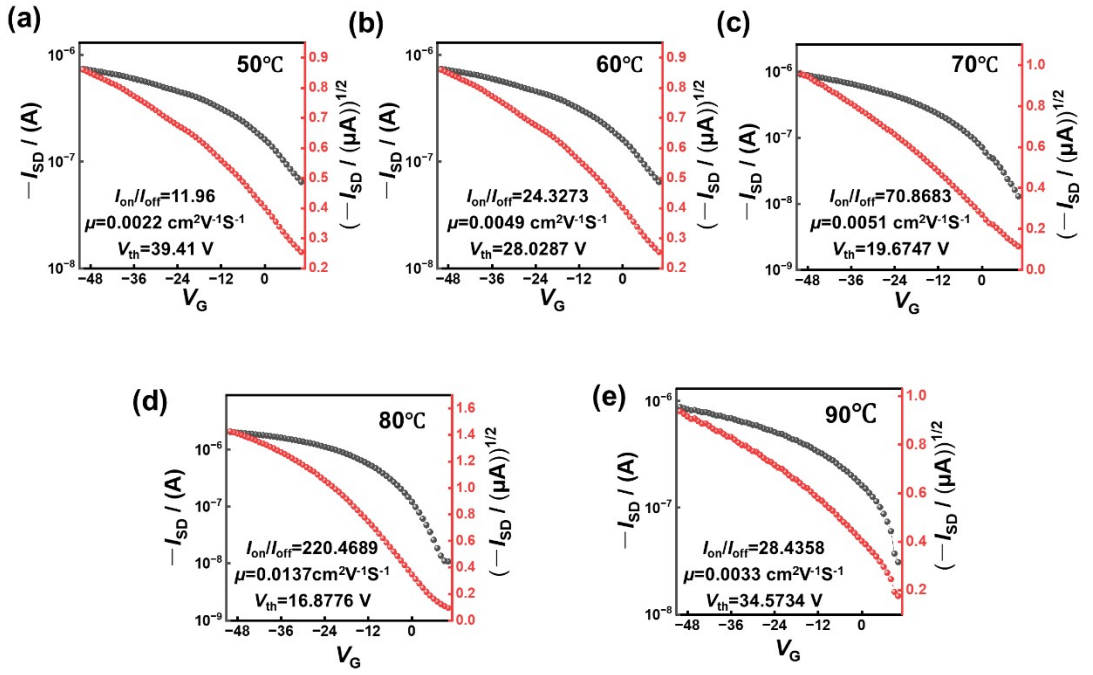

Fig. S5. Transfer curves of different dissolution temperatures on the OTFTs based on P3HT NW. (a) 50°C, (b) 60°C, (c) 70°C, (d) 80°C, and (e) 90°C.

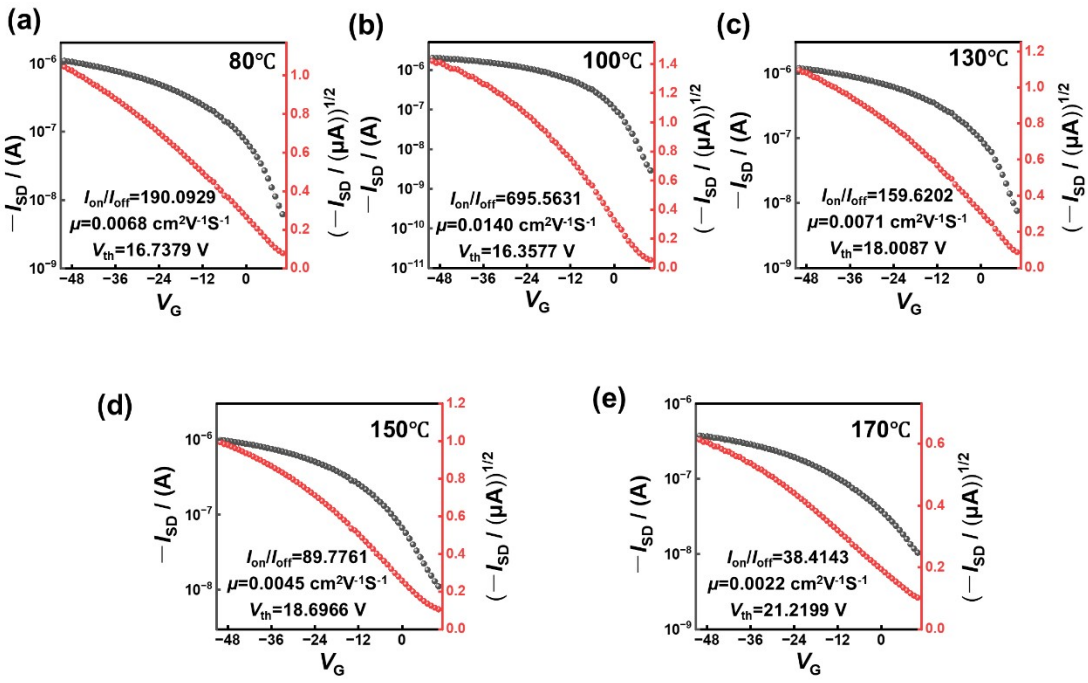

Fig. S6. Transfer curves of different annealing temperatures on the OTFTs based on P3HT NW. (a) 80°C, (b) 100°C, (c) 130°C, (d) 150°C, and (e) 170°C.

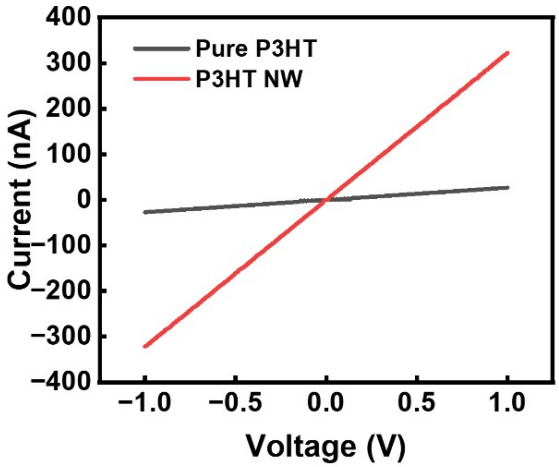

Fig. S7. Comparison of *I-V* curves for pure P3HT and P3HT NW.

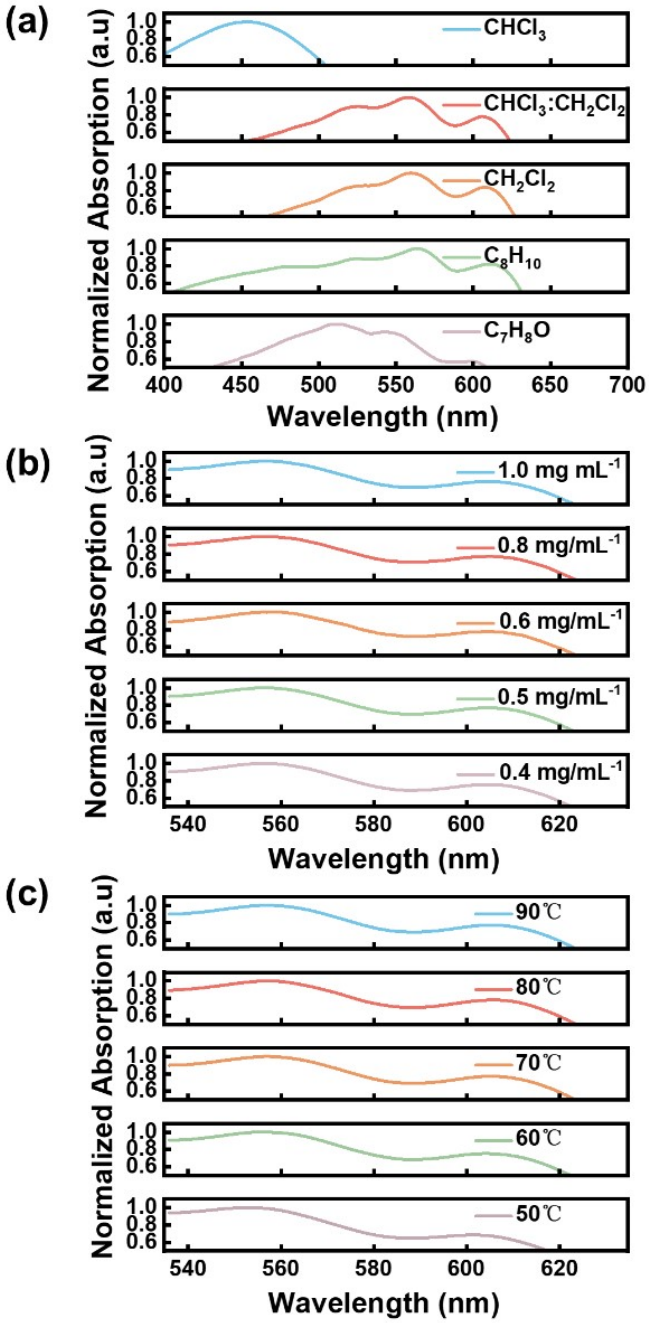

Fig. S8. Normalised UV-vis spectroscopy of P3HT under different preparation conditions. (a) variation in absorption spectra across different solvent. (chloroform, chloroform and dichloromethane, dichloromethane, p-xylene, and anisole), (b) variation in absorption spectra across different concentrations (0.4 mg mL^{-1}, 0.5 mg mL^{-1}, 0.6 mg mL^{-1}, 0.8 mg mL^{-1}, and 1.0 mg mL^{-1}), (c) variation in absorption spectra across different dissolution temperatures (50°C, 60°C, 70°C, 80°C, and 90°C).

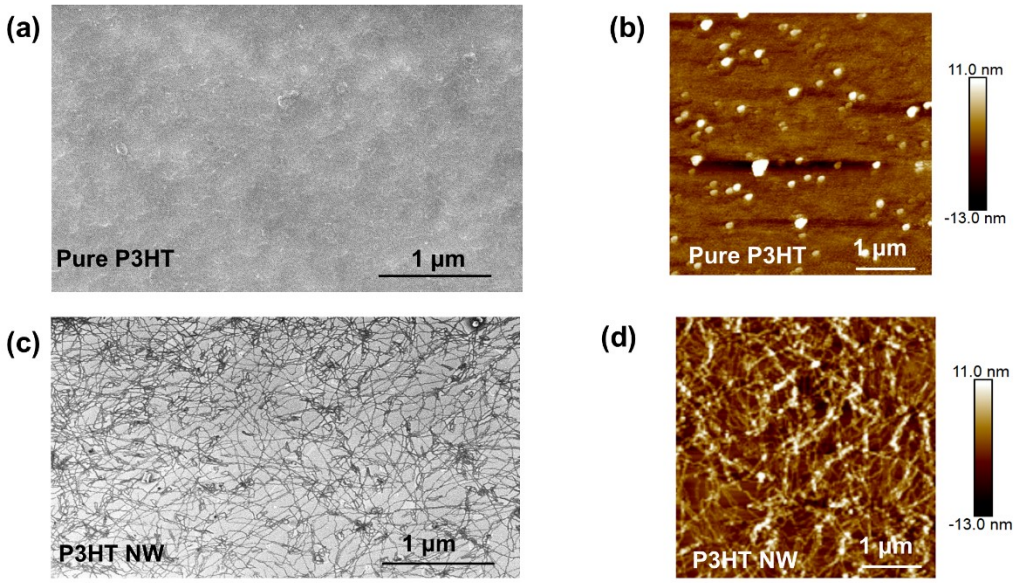

Fig. S9. Microscopic morphology of the pure P3HT film and the P3HT NW film. (a) SEM image of the pure P3HT film, (b) AFM image of the pure P3HT film, (c) SEM image of the P3HT NW film, (d) AFM image of the P3HT NW film.

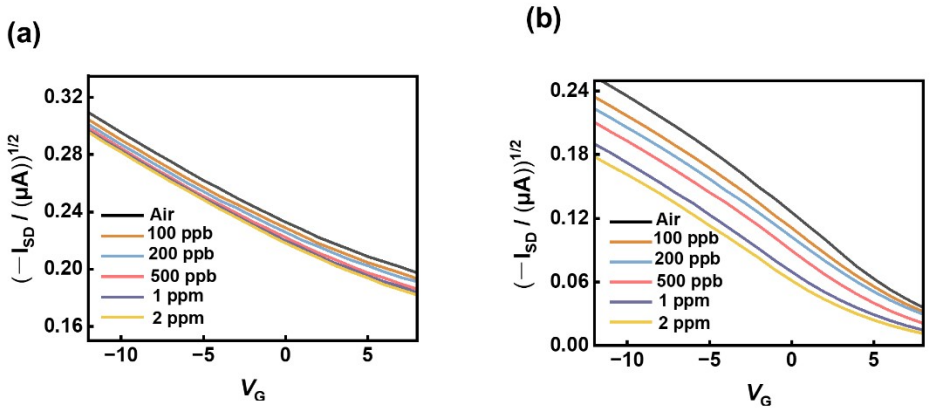

Fig. S10. Variation of square root coordinates in transfer curves at different NH_3 concentrations. (a) OTFTs based on pure P3HT film, (b) OTFTs based on P3HT NW.

Experimental parameters based on electrochemical test CV curves

CV curve testing was conducted in a standard three-electrode system at room temperature. The experiment employed a platinum plate modified with either pure P3HT or P3HT NW served as the working electrode, while a platinum wire and an Ag/AgCl electrode functioned as the counter and reference electrodes, respectively. The electrolyte system consisted of 0.1 mol/L PBS solution. To ensure device performance reached a stable state and to eliminate potential interference from irreversible processes during the initial scan, each sample underwent six consecutive cyclic voltammetry scans at a scan rate of 0.05 V s^{-1}. Data from the second scan were specifically selected for plotting CV curves and subsequent surface adsorption energy calculations. All electrochemical data reported herein were based on repeated measurements from at least three independent devices to ensure data reliability and reproducibility. Furthermore, calculations involving performance parameters such as electrochemically active surface coverage were uniformly normalized based on the working electrode's geometric area (0.01 cm^2).

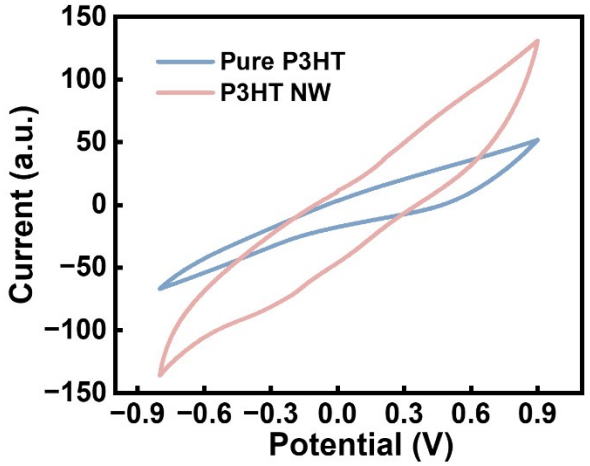

Fig. S11. Comparison of CV curves between the pure P3HT film and the P3HT NW film (for calculating electrochemical surface area).

Table S1. Comparison of P3HT-based ammonia sensor with other reported works.

Materials	LOD/lowest tested concentration	NH_3 concentration	Response	Selectivity test	ML	Reference
P3HT/PS	Not reported /5 ppm	5 ppm	16.9%	H_2S, NO_2, SO_2	NO	[1]
P3HT-ZnO nanorods	Not reported /1 ppm	5 ppm	19.3%	CO, NO_2, H_2S	NO	[2]
P3HT/SWCNTs	Not reported /5 ppm	5 ppm	11.2%	Not reported	NO	[3]
P3HT/TPFB	Not reported /10 ppm	10 ppm	17.0%	Acetone, methanol, DCM, H_2O vapor	NO	[4]
P3HT-rGO-MWCNT	Not reported /10 ppm	10 ppm	3.6%	Not reported	NO	[5]
P3HT/PMMA	Not reported /10 ppm	10 ppm	31.1%	Acetone，ethanol, Ether, ethyl acetate, Toluene	NO	[6]
P3HT/GO	278 ppb/5 ppm	5 ppm	13.4%	CO, CO_2, CH_4, Ethylene	NO	[7]
P3HT/MoS_2	904 ppb/10 ppm	10 ppm	18.2%	CH_4, CO, CO_2	NO	[8]
P3HT	1 ppm/10 ppm	10 ppm	17.7%	Not reported	NO	[9]
P3HT	Not reported /67 ppm	67 ppm	16.6%	H_2O, methanol, acetone, $CHCl_3$	NO	[10]
P3HT nanowire	238 ppb/100 ppb	2 ppm	20.3%	Toluene, ethanol, SO_2, formaldehyde, Cl_2, NO_2	Yes	This work

Notes and references

[1] S. Han, X. Zhuang, W. Shi, X. Yang, L. Li and J. Yu, *Sens. Actuators, B*, 2016, **225**, 10-15.

[2] K. X. Han, C. C. Wu, W. F. Hsu, W. Chien and C. F. Yang, *Synth. Met*., 2023, **299**, 117449.

[3]A. Nijkoops, M. Ciocca, S. Krik, A. Douaki, A. Gurusekaran, S. Vasquez, M. Petrelli, M. A. C. Angeli, L. Petti and P. Lugli, *lsens.*, 2023, **7**, 1-4.

[4] A. A. Meresa and F. S. Kim, *Polymers*, 2020, **12**, 128.

[5] T. S. T. Khanh, T. Q. Trung, L. T. T. Giang, T. Q. Nguyen, N. D. Lam and N. N. Dinh, *Appl. Sci.*, 2021, **11**, 6675.

[6] X. Wang, Z. Liu, S. Wei, F. Ge, L. Liu, G. Zhang, Y. Ding and L. Qiu, *Synth. Met*., 2018, **244**, 20-26.

[7] A. Verma, P. Kumar, V. K. Singh, V. N. Mishra and R. Prakash, *Sens. Actuators, B*, 2023, **385**, 133661.

[8] A. Verma, P. K. Sahu, V. Chaudhary, A. K. Singh, V. N. Mishra and R. Prakash, *IEEE Sens. J.*, 2022, **22**, 10361-10369.

[9] M. S. Park, A. A. Meresa, C. M. Kwon and F. S. Kim, *Polymers*, 2019, **11**, 1682.

[10] M. R. Cavallari, J. E. Izquierdo, G. S. Braga, E. A. Dirani, M. A. Pereira-da-Silva, E. F. Rodriguez and F. J. Fonseca, *Sensors*, 2015, **15**, 9592-9609.